Multi-channel Implementation of Semi-Adiabatic Excitation Pulses

Marcin Jankiewicz[1] and Jay Moore[2]

[1]MRC/UCT Medical Imaging Research Unit, Department of Human Biology, University of Cape Town, Observatory, Western Cape, South Africa, [2]Department of Radiology and Radiological Sciences, Vanderbilt University, Nashville, TN, United States

Target Audience

Imaging scientists interested in pulse design, parallel transmission and adiabatic pulses.

Purpose

The problem of inhomogeneous RF transmission (B_1^+) fields in high-field MRI has previously been addressed by various RF pulse designs (e.g. sparse spokes [1], adiabatic pulses [2,3], and composite pulses [4,5]) and hardware modifications (e.g. parallel transmit coils [6], load-insensitive coils [7], and travelling-wave antennae [8]). We show a construction that enables the design and implementation of semi-adiabatic waveforms with performance optimized on a grid of predefined (complex $B_1^+)_i$ (i=1, …, p) and Δf_0 values associated with a p-channel transmission system. Optimization is performed such that the j-th channel takes into consideration the existence of the RF output from the other p-1 channels. Results are illustrated on a dual ptx setup (p=2), and improvements are demonstrated relative to similar single-channel designs.

Methods

The optimization grid S for a 2-channel system can be written as a direct sum of vector products of $B_1^+ \otimes \Delta f_0$ spaces, i.e., $S = [S_1 \otimes S_3] \oplus [S_2 \otimes S_3]$, where S_1 and S_2 represent B_1^+ inhomogeneities (complex, i.e. amplitude and relative phase) of channels 1 and 2 of the dual transmit system and S_3 is the Δf_0 space spanned by a user specified range of static field inhomogeneities (in Hz). A schematic of the optimization space is presented in Fig. 1. We have considered two classes of pulses: (i) pulses utilizing maximal available RF amplitude (RF_{max}) on both channels; and (ii) pulses utilizing only ½RF_{max}. In accordance with the limitations of typical 7 T human imaging system, RF_{max} was taken to be 15μT. These composite pulses are characterized by a number of sub-pulses (*numsp*) and the duration of each sub-pulse (*numdt* in units of a 6.4μs dwell time: 7T Philips Achieva scanner (Philips Healthcare, Cleveland, Ohio, USA)). A wide range of such pulse structures were tested (*numsp*=1,…,20 and *numdt*=1,…,20), resulting in 400 distinct dual-pulse trains for each of the two maximum amplitude categories. The amplitude and phase modulated RF trains (RF_1(t) acting on $S_1 \otimes S_3$ and RF_2(t) acting on $S_2 \otimes S_3$) are optimized simultaneously in space S with identical S_1 and S_2 defined by a typical ranges of inhomogeneities in a human brain at 7 T ($B_1^+/(B_1^+{}_{nom}=45^o)$=0.3-1 and a range of relative phases between channels 1 and 2 (0^o-90^o); Δf_0 = ±250Hz) in a similar fashion to the scheme presented in [5]. The effect of each pulse train was simulated using field maps measured in a single axial slice of a human head phantom at 7 T (with $B_1^+/B_1^+{}_{nom}$ and Δf_0 values falling within a range specified above). To aid in determining any inherent advantage in this multi-channel implementation, similar pulse optimizations were performed (*numsp*=1,…,20 and *numdt*=1,…,40) using 7 T single-channel field maps for the same slice of the head phantom and an amplitude limit equal to RF_{max}, thus resulting in a total of 800 single-channel pulses. In order to quantify performance, percent error maps (% deviations from the mean $B_1^+/(B_1^+{}_{nom}=45^o)$) were calculated for each pulse in each of the three classifications (i.e., single-channel pulses and two classes of dual-channel pulses).

Results

Figure 2 shows the % error values for the 800 single-channel optimized pulses (top), and the two classes of 400 different dual-channel pulses. The dotted line (grey dots) on each plot designates the isochrones corresponding to total pulse duration of 1ms.

Discussion

Even for the second class of pulses, for which the RF amplitude is constrained to ½RF_{max}., the performance gain over single-channel waveforms is noticeable (Fig. 2). This gain is a result of doubling the number of degrees-of-freedom available to the optimization for any given pulse duration. In general, the same performance can be attained with The performance of the higher amplitude class of dual-channel pulses is significantly better than that of the single-channel class given that the same level of flip-angle homogeneity is achievable in half the time.

Conclusion

To our knowledge this is the first attempt to develop a construction of amplitude- and phase-modulated composite pulses on a multi-channel system. Generalization of this construction to p transmit-channels is straightforward and requires extension of the optimization space S to p versions of $[(B_1^+)_1 \times \Delta f_0]$ spaces.

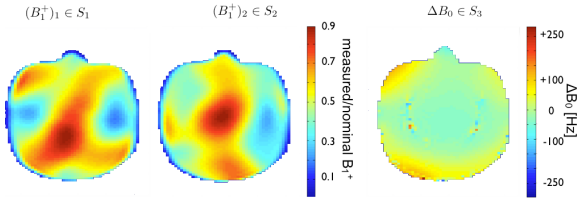

$$S = (S_1 \oplus S_2) \otimes S_3$$
$$S = (S_1 \otimes S_3) \oplus (S_2 \otimes S_3)$$

when solving Bloch equations in the optimization space:

$$\hat{B}^+_{1ijk}(t) = \hat{B}^+_{1ik} RF_1(t) + \hat{B}^+_{1jk} RF_2(t)$$
$$i \in S_1,\ j \in S_2,\ k \in S_3$$

Fig.1: Schematic of the optimization space S for a dual-transmit channel system. The amplitude and phase modulated waveforms RF_1(t) and RF_2(t) act on spins in different spaces $[S_1 \otimes S_3]$ and $[S_2 \otimes S_3]$, correspondingly. Their combined performance in the final space S is the results of interaction of these two waveforms at each point in time during their execution.

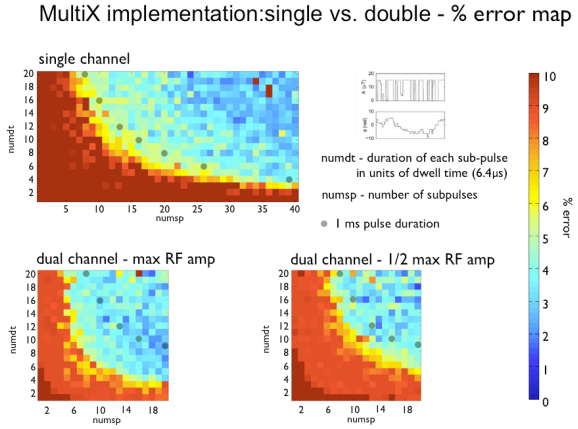

Fig.2: Comparison of performances of single- and dual-channel implementations of amplitude and phase modulated pulses. Each pixel corresponds to a mean percent error calculated for the central axial slice of a single/dual B_1^+ map of the same human head phantom. For the dual channel simulations two classes of pulses were generated. The first class utilized maximal available RF amplitude on both channels; the second class utilized half of the available amplitude. Notice that performance similar to the single-channel implementation can be achieved for the second class of pulses but in half the time. Grey dots mark a 1 ms pulse duration.

References [1] Zelinski A., et al. Magn Reson Med 2008; 59:1355-1364. [2] Staewen RS, et al. Investigative Radiology 1990; 25:559-567. [3] Wiesinger F., Boesiger P, Pruessmann KP. Magn Reson Med 2004; 52:376-390. [4] Skinner TJ, et al. J Magn Reson 2003; 163:8-15. [5] Moore J, M. Jankiewicz, H. Zeng, A.W. Anderson, J.C. Gore, ``Composite RF pulses for B_1^+ -insensitive volume excitation at 7 Tesla", Journal of Magnetic Resonance, 205, 50, 2010. [6] Hornak JP, Szumowski J, Bryant RG. Magn Reson Med 1988; 6:158-163. [7] Ibrahim TS, et al. in Proc ISMRM 2008; 438. [8] Brunner D, et al. Nature 2009; 457:994-998.